MEDWIN PUBLISHERS
Committed to create value for Researchers

Nanomedicine & Nanotechnology Open Access
ISSN: 2574-187X

Consciousness Energy Healing Treatment and Its Effect on the Structural Properties and Isotopic Abundance Ratio of Tetrahydrocurcumin

Mahendra KT[1] and Snehasis J[2]*

[1]Trivedi Global, Inc., Henderson, USA

[2]Trivedi Science Research Laboratory Pvt. Ltd., Thane (W), India

***Corresponding author**: Snehasis Jana, Trivedi Science Research Laboratory Pvt. Ltd, Thane (W), Maharashtra, India, Email: publication@trivedieffect.com

Research Article

Volume 4 Issue 4

Received Date: November 19, 2019

Published Date: December 17, 2019

DOI: 10.23880/nnoa-16000171

Abstract

Tetrahydrocurcumin (THC) is being studied for the prevention and treatment of various diseases. The aim of this study was to investigate the effect of the Trivedi Effect®-Biofield Energy Healing Treatment on the structural properties and isotopic abundance ratio of THC using sophisticated spectroscopy methods. THC sample was divided into two parts. One part of THC did not receive the Biofield Treatment called control sample. The second part of the THC was treated with the Biofield Energy Treatment remotely by a renowned Biofield Energy Healer, Mr. Mahendra Kumar Trivedi is known as treated sample. The spectroscopy studies confirmed the structure of tetrahydrocurcuminoids, and the sample majorly contains THC. The gas chromatography-mass spectrometry spectra of the control and treated THC showed with the molecular ion at *m/z* 372.2 $(C_{21}H_{24}O_6)^+$ and the isotopic abundance ratio of P_{M+1}/P_M in the treated sample was increased by 2.12% compared with the control sample. Thus, the contributions of ^{13}C, ^{2}H, and ^{17}O from $(C_{21}H_{24}O_6)^+$ to *m/z* 373.2 in the treated sample were increased compared with the control sample. The liquid chromatography-mass spectrometry of both the sample exhibited three major peaks at R_t of 16.1, 17.3, and 17.48 minutes confirmed the presence of one diketo form and two enol form of THC, respectively. The peak area% of the treated THC at R_t of 16.1 and 17.5 minutes were increased by 1.62% and 0.68% respectively, whereas, at R_t of 17.30 minutes, it was decreased by 8.10% compared with the control sample. Similarly, the relative mass peak intensities of the treated THC at R_t of 16.1 and 17.3 minutes were significantly increased by 17.79% and 80.81% respectively, but at R_t of 17.5 minutes, it was decreased by 8.10% compared with the control sample. It can be assumed that the relative concentration of the treated THC was altered compared with the control sample. Thus, the Trivedi Effect®-Consciousness Energy Healing Treated THC with altered isotopic abundance ratio and relative concentration might have altered the physicochemical properties compared to the

untreated THC. The treated THC would be very useful to design better nutraceutical/pharmaceutical formulations which might offer better therapeutic response against cancer, arthritis, dementia, diabetes, hepatotoxicity, etc.

Keywords: Tetrahydrocurcumin; The Trivedi Effect®; Biofield Energy; Consciousness Energy Healing Treatment; Isotopic abundance; Peak area; LC-MS; GC-MS

Introduction

Tetrahydrocurcumin (THC) is a major metabolite of curcumin, which is colourless/white polyphenolic compound with similar biochemical and physiological actions of curcumin [1,2]. THC is being studied for the treatment of cancer, dementia, and shown to have protective effects against diabetes and vascular dysfunction. It has strong antioxidant and anti-inflammatory properties to those of other naturally occurring curcuminoids, including curcumin, demethoxycurcumin, and bisdemethoxycurcumin [2-5]. In comparison to the curcumin, THC has different molecular targets, signalling pathways, cellular responses, and clinically more advantageous [2-5]. Many studies also reported that THC has significant results in preventing hepatotoxicity, nephrotoxicity, rheumatoid arthritis, the ageing process, atherosclerotic lesions, etc. [2-7]. It has a remarkable role in angiogenesis and also improves the accumulation of extracellular matrix components through the remodeling of the wound repair [5]. However, THC did not show any associated toxicity even at higher doses and can be used against tumors of the skin, colon, pancreas, breast, psoriasis, and scleroderma [5,7].

The chemical structure of the THC so far characterized are available in three different forms such as one diketo form, and two enol tautomeric form (Figure 1) [8]. THC is poorly soluble even in hot water and soluble in the organic solvents like alcohol, acetone, and glacial acetic acid. Thus, the pharmacological effect of THC is limited due to its poor aqueous solubility. In addition, due to relatively short gastric emptying time results in an incomplete release of THC from the dosage form at the site of absorption and lead to a lower efficacy of the administered dose [9]. The half-lives of THC found to be 813 minutes in cell culture medium and 232 minutes in plasma [2]. However, many studies conducted on the bioavailability of THC and was found better bioavailable in the intestine, brain, hepatic cytosol, *etc.* compared to the curcumin but neither THC nor curcumin was detected in the plasma of mice [10].

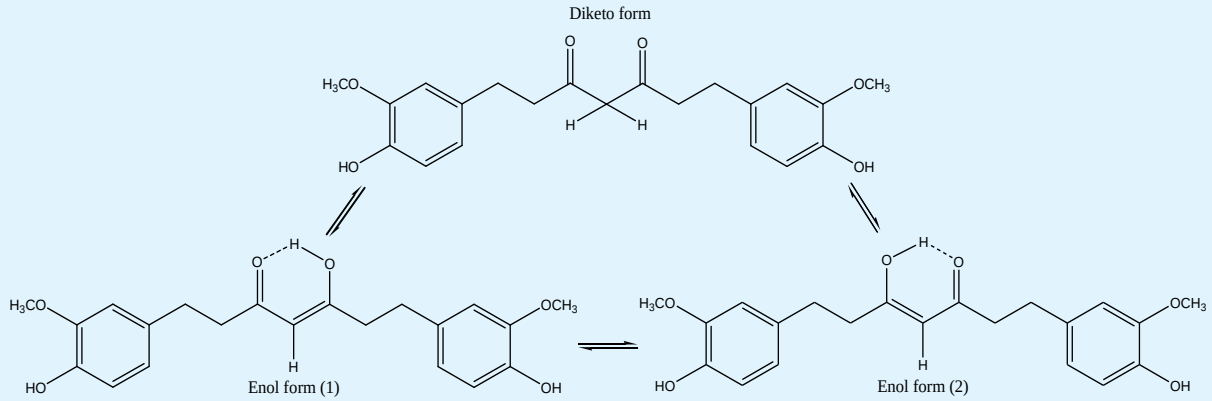

Figure 1: Structure of tetrahydrocurcumin with diketo and two enol resonance form.

Better solubility and bioavailability in the physiological fluid system are the major issue for THC. The Biofield Energy Treatment (the Trivedi Effect®-Consciousness Energy Healing Treatment) could be an economical approach for the improvement of the solubility and bioavailability by reducing the crystallite size, particle size, and improvement of the surface area of THC [11,12]. The human body can discharge the electromagnetic waves in the form of bio-photons that surrounds the body. This electromagnetic energy is generated by the continuous movement of electrically charged particles (ions, cells, etc.) inside the body collectively known as "Biofield Energy". Biofield Energy Healers have the ability to harness the energy from the environment or "Universal Energy Field" and can transmit into any living or non-living object(s). The process by which objects receive the Biofield Energy and respond into a useful way is called Biofield Energy Healing Treatment/ Consciousness Energy Healing Treatment [13-15]. Biofield based Energy Therapies are used worldwide to promote health and healing. National Center of Complementary and Integrative Health (NCCIH) has recognized and accepted Biofield Energy Healing as a Complementary and Alternative Medicine (CAM) health care approach in addition to other therapies, medicines and practices such as natural products, Ayurvedic medicine, Chinese herbs and medicines, aromatherapy, essential oils, homeopathy, yoga, meditation, deep breathing, Qi Gong, Tai Chi, chiropractic and osteopathic manipulation, special diets, massage, progressive relaxation, guided imagery, acupressure, acupuncture, relaxation techniques, Reiki, healing touch, hypnotherapy, movement therapy, rolfing structural integration, pilates, mindfulness, naturopathy, traditional cranial sacral therapy and applied prayer (as is common in all religions, like Christianity, Hinduism, Buddhism, Judaism, etc.) [16]. The Biofield Energy Healing Treatment had been expansively reported with significant results in different scientific fields like agricultural science [17-19], microbiology [20-23], genetics [24,25], cancer research [26,27], materials science [11,12,28-30], pharmaceutical science [31-33], etc. Some of the scientific studies indicated that the Trivedi Effect®-Consciousness Energy Healing Treatment altered the natural isotopic abundance ratio of the substances [34,35]. Such alteration of the atom/ion may be due to the Trivedi Effect®-Consciousness Energy Healing Treatment through the possible mediation of neutrinos [36]. The stable isotope ratio analysis has various applications in different scientific fields for understanding the isotope effects resulting from the variation of the isotopic composition of the molecule [37,38]. Conventional mass spectrometry (MS) techniques such as gas chromatography - mass spectrometry (GC-MS) and liquid chromatography - mass spectrometry (LC-MS), are widely used for isotope ratio analysis in low micromolar concentration with sufficient precision [35,37]. Hence, GC-MS, LC-MS, and NMR (Nuclear Magnetic Resonance) were used in this study to characterize the structural properties of the Biofield Energy Treated and untreated THC. Consequently, GC-MS based isotopic abundance ratio analysis of P_{M+1}/P_M ($^2H/^1H$ or $^{13}C/^{12}C$ or $^{17}O/^{16}O$) in both of the treated and untreated samples were aimed to investigate the impact of the Trivedi Effect® - Consciousness Energy Healing Treatment on the isotopic abundance ratio in THC.

Materials and Methods

Chemicals and Reagents

The test sample tetrahydrocurcumin was purchased from Novel Nutrient. Pvt. Ltd., India. The HPLC grade acetonitrile, methanol, formic acid were purchased from Merck, India. Milli Q® water was procured from Evoqua, India.

Consciousness Energy Healing Treatment Strategies

The test sample of THC was divided into two parts. One part of THC did not receive the Biofield Energy Treatment known as a control sample. The second part of THC was received the Trivedi Effect®-Consciousness Energy Healing Treatment remotely under standard laboratory conditions for 3 minutes by a famous Biofield Energy Healer, Mr. Mahendra Kumar Trivedi (USA) and known as the Biofield Energy Treated THC. Further, the control group was treated with a "sham" healer who did not have any knowledge about the Biofield Energy Treatment. After that, both the samples were kept in sealed conditions and characterized using GC-MS, LC-MS, and NMR analytical techniques.

Characterization

Gas Chromatography-Mass Spectrometry (GC-MS) Analysis and Calculation of Isotopic Abundance Ratio

The GC-MS of the control and Biofield Energy Treated sample were analyzed with the help of Agilent 7890B Gas chromatograph equipped with a 30 m x 0.25 mm i.d., silica capillary column (HP-5 MS) and coupled to a quadrupole detector with pre-filter (5977B, USA) was

operated with electron impact (EI) ionization in positive mode at 70 eV. Oven temperature was programmed from 50 °C (1 min hold) to 150 °C @ 20 °C /min to 200 °C (6 min hold) @ 25 °C /min (12 min hold). The identification of analyte was made by GC retention times and by a comparison of the mass spectra of samples.

The natural abundance of each isotope (C, O, and H) can be predicted from the comparison of the height of the isotope peak with respect to the base peak. The values of the natural isotopic abundance of the common elements are obtained from several kinds of literature [38-42]. The change in isotopic abundance ratio (P_{M+1}/P_M) of the Biofield Energy Treated THC was calculated compared with the control sample using equation 1.

% change in isotopic abundance ratio = [(Treated – Control)/ Control] x 100 (1)

Liquid Chromatography-Mass Spectrometry (LC-MS) Analysis

The LC-MS analysis of the control and Biofield Energy Treated THC was carried out with the help of LC-Dionex Ultimate 3000, MS-TSQ Endura, USA equipped with a photo-diode array (PDA) detector connected with a triple-stage quadrupole mass spectrometer (Thermo Scientific TSQ Endura, USA) with a Thermo Scientific Ion Max NG source and heated electrospray ionization (ESI) probe. The column used here was a reversed phase Zorbax SB-C18 100X4.6mm, 3.5µm, maintained at 40˚C. 10 µL of THC solution in methanol was injected and the analyte was eluted using 2 mM ammonium formate in water with 0.5% formic acid (mobile phase A) and acetonitrile (mobile phase B) pumped at a constant flow rate of 0.6 mL/min. Chromatographic separation was achieved using gradient condition as follow: 0.1 min-5%B, 5.0 min-5%B, 15.0 min-75%, 20.0 min-75%B, 25.0 min-95%B, 30.0 min-95%B, 35.0 min-5%B and 40.0 min-5% B and the total run time was 40 min. Peaks were monitored at 280 nm using the PDA detector. The mass spectrometric analysis was performed under positive ESI mode. The total ion chromatogram, peak area% and mass spectrum of the individual peak, which was appeared in LC along with the full scan were recorded.

The percent change in LC peak area% (P) and mass peak intensity (I) was calculated using the following equation 1.

Nuclear Magnetic Resonance (NMR) Analysis

^1H and ^{13}C NMR analysis of the control and Biofield Energy Treated THC were conducted at 400 MHz and 100 MHz, respectively on an Agilent-MRDD2 FT-NMR spectrometer at room temperature using TMS as an internal standard. Chemical shifts (δ) were in parts per million (ppm) relative to the solvent's residual proton chemical shift (DMSO-d_6, δ = 2.50 ppm) and solvent's residual carbon chemical shift (DMSO-d_6, δ = 39.52 ppm).

Results and Discussion

Gas Chromatography-Mass Spectrometry (GC-MS) Analysis and Calculation of

Isotopic Abundance Ratio

The GC chromatograms and mass spectra of both the samples of THC are shown in Figures 2 and 3, respectively. The GC chromatogram of the control THC revealed the presence of two peaks at the retention time (R_t) 23.85 and 25.46 min with the peak percentage (%) area of 3.32 and 96.68%, respectively (Figure 2). Consequently, these two peaks were observed in the GC chromatogram of the Biofield Energy Treated THC at the retention time 23.98 and 25.57 min with the peak percentage (%) area of 2.93 and 97.07%, respectively (Figure 2). This finding indicated that the polarity of the Biofield Energy Treated THC was remained unaltered compared to the control sample.

The mass spectra of the control and Biofield Energy Treated samples (Figures 3a and b) at the retention time 23.85 and 23.98 min, respectively displayed the mass for demethoxy THC at *m/z* 342.1 $[M]^+$ (calcd for $C_{20}H_{22}O_5^+$, 342.1) along with the fragment ion peaks at *m/z* 150.1, 137.1, 122.0, 107.1 and 77.1 which were corresponded to the molecular formula $C_9H_{10}O_2^{+\bullet}$, $C_8H_9O_2^+$, $C_8H_8O^+$, $C_7H_7O^+$, and $C_6H_5^+$, respectively (Figure 4). The mass spectra of the control and Biofield Energy Treated samples of THC (Figures 3c and d) at the retention time 25.46 and 25.57 min, respectively exhibited the molecular mass for THC at *m/z* 372.2 $[M]^+$ (calcd for $C_{21}H_{24}O_6^+$, 372.2) along with the fragment ion peak at *m/z* 137.1 corresponded to the molecular formula $C_8H_9O_2^+$ that showed 100% relative peak intensity (Figure 4).

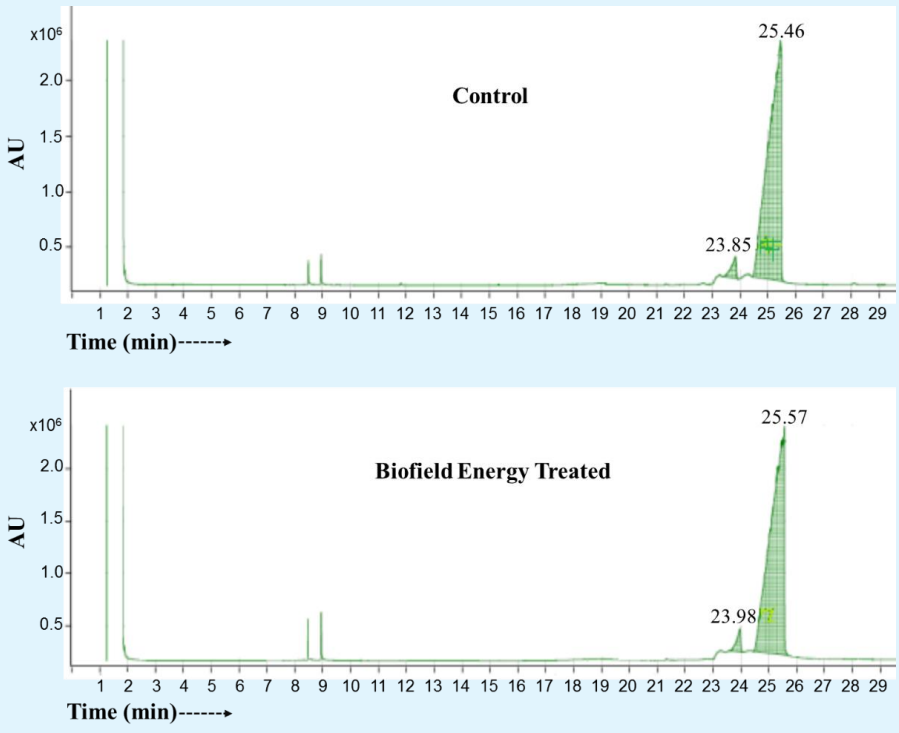

Figure 2: Gas chromatograms of *the control and Biofield Energy Treated* THC.

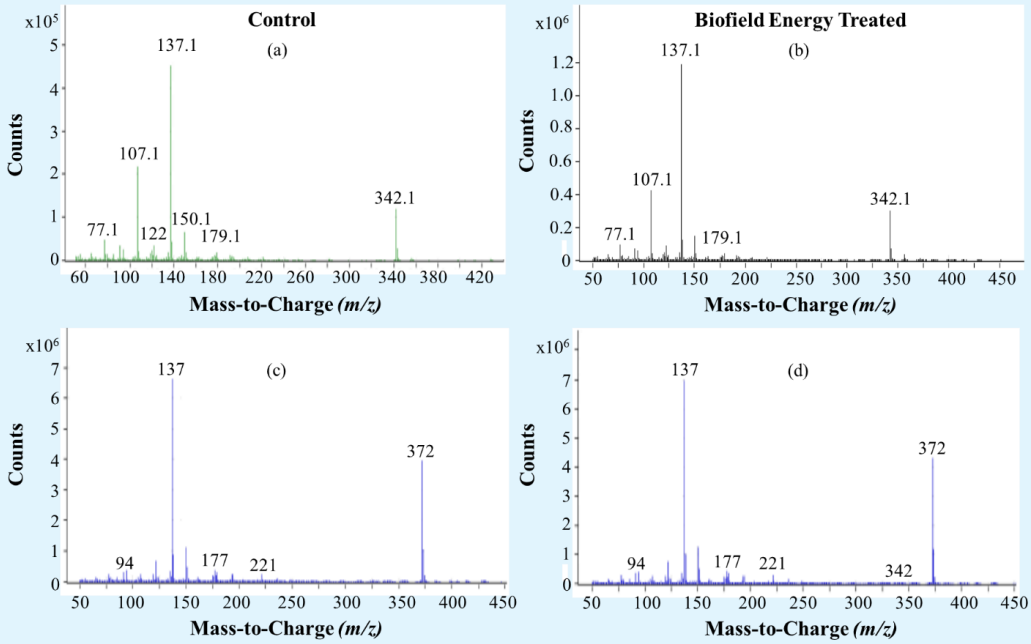

Figure 3: Mass spectra of *the control* THC *at* R_t *23.85 min (a), 23.98 min (c) and Biofield Energy Treated* THC *at* R_t *25.46 min (b), 25.57 min (d).*

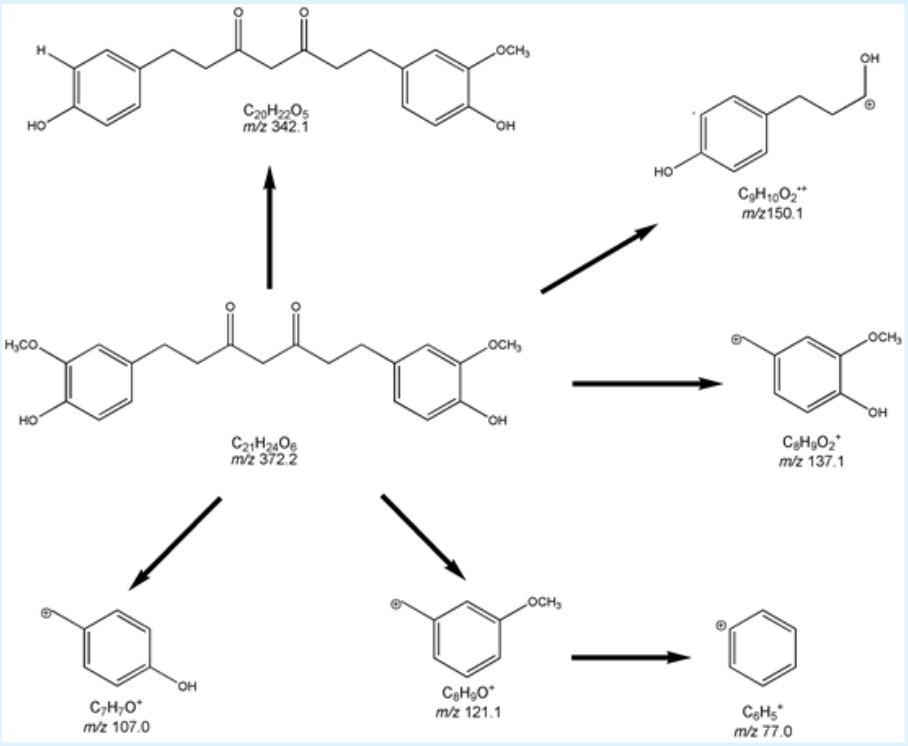

Figure 4: Proposed fragmentation pathway of THC.

The MS spectra of the control and Biofield Energy Treated THC showed the mass of the molecular ion at *m/z* 372.2 $(C_{21}H_{24}O_6)^+$ showing relative intensity of 59.55% and 61.77%, respectively. The theoretical calculation of P_{M+1} for THC was presented as below:

P (^{13}C) = [(21 x 1.1%) x 59.55% (the actual size of the M^+ peak)] / 100% = 13.76%

P (^{2}H) = [(24 x 0.015%) x 59.55%] / 100%= 0.21%

P (^{17}O) = [(6 x 0.04%) x 59.55%] / 100% = 0.14%

P_{M+1}, *i.e.* ^{13}C, ^{2}H, and ^{17}O contributions from $(C_{21}H_{24}O_6)^+$ to *m/z* 373.2 = 14.11%

From the above calculation, it has been found that ^{13}C and ^{17}O have major contribution to *m/z* 373.2. The experimental P_{M+1} data of THC showed the close value to the calculated value.

The isotopic abundance ratio analysis of THC in control and Biofield Energy Treated samples were calculated for its molecular mass at *m/z* 372.2. P_M and P_{M+1} for THC at *m/z* 372.2 and 373.2, respectively of the control and Biofield Energy Treated samples were obtained from the observed relative mass peak intensities of $[M^+]$ and $[(M+1)^+]$ peaks, respectively in the ESI-MS spectra and are presented in Table 1.

Parameter	Control	Biofield Energy Treated
P_M at *m/z* 372.2 (%)	59.55	61.77
P_{M+1} at *m/z* 373.2 (%)	15.68	16.61
P_{M+1}/P_M	0.2633	0.2689
% Change of isotopic abundance ratio (P_{M+1}/P_M) with respect to the control sample		2.12

Table 1: *Isotopic abundance analysis results of tetrahydrocurcumin in control and Biofield Energy Treated samples.* P_M: the relative peak intensity of the parent molecular ion $[M^+]$; P_{M+1}: the relative peak intensity of the isotopic molecular ion $[(M+1)^+]$, and M: mass of the parent molecule.

The percentage change of the isotopic abundance ratios (P_{M+1}/P_M) in the Biofield Energy Treated sample compared with the control sample is shown in Table 1. The isotopic abundance ratio of P_{M+1}/P_M in the Biofield Energy Treated sample was increased by 2.12% compared with the control sample (Table 1). So, ^{13}C, ^{2}H, and ^{17}O, contributions from $(C_{21}H_{24}O_6)^+$ to *m/z* 373.2 in the Biofield Energy Treated sample were increased compared with the control sample.

Liquid Chromatography-Mass Spectrometry (LC-MS) Analysis

The LC chromatograms of the control and Biofield Energy Treated samples of tetrahydrocurcumin showed the presence of six peaks near the retention time (R_t) of 14.7, 15.2, 15.9, 16.1, 17.3, and 17.5 minutes (Figures 5). These six peaks indicated the presence of tetrahydrocurcuminoids and were proposed with the help of ESI mass spectra of THC (Figure 6). Octahydrocurcumin (OHC) was proposed from the chromatographic peak at R_t of 14.7 minutes, which exhibited the mass of the molecular ion adduct with sodium at *m/z* 398.93 $[M + Na]^+$ (calculated for $C_{21}H_{32}O_6Na^+$, 399.18) in the control sample and at *m/z* 399.37 $[M + Na]^+$ in the Biofield Energy Treated sample. The fragment ion peaks at *m/z* 341.32 and 341.23 (base peak) corresponded to the molecular formula $C_{21}H_{26}O_4^{2+}$ (Figure 6) in control and Biofield Energy Treated samples, respectively supported the structure of OHC. The chromatographic peak area% of OHC was decreased by 8.05%, whereas the mass peak intensity was significantly increased by 152.29% (Table 2). The mass spectrum of the control and Biofield Energy Treated THC shown the presence of the molecular mass of hexahydrocurcumin (HHC) at *m/z* 398.38 $[M + Na + H]^+$ (calculated for $C_{21}H_{27}O_6Na^+$, 398.17) and at *m/z* 397.32 $[M + Na]^+$ (calculated for $C_{21}H_{26}O_6Na^+$, 397.16), respectively the at R_t of 15.2 minutes (Figure 6). The fragment ion peak at *m/z* 357.33 and 357.02 (base peak) in control and Biofield Energy Treated samples, respectively correspond to the molecular formula $C_{21}H_{24}O_4^{2+}$ supported the structure of HHC. The chromatographic peak area% of HHC was decreased by 0.71%, whereas the mass peak intensity was significantly increased by 368.83% (Table 2). Similarly, tetrahydrodemethoxycurcumin (THDC) was proposed at the retention time of 15.9 minutes showed the protonated mass at *m/z* 343.36 $[M + H]^+$ (calculated for $C_{20}H_{23}O_5^+$, 343.15) in the control sample and at *m/z* 343.06 $[M + H]^+$ in the Biofield Energy Treated sample. The major fragment ion peak at *m/z* 325.14 and 325.74 (base peak) in control and Biofield Energy Treated sample, respectively were corresponding to the molecular formula $C_{20}H_{21}O_4^+$ supported the structure of THDC (Figure 6). The chromatographic peak area% and the mass peak intensity of THDC were increased by 5.38% and 17.79% (Table 2).

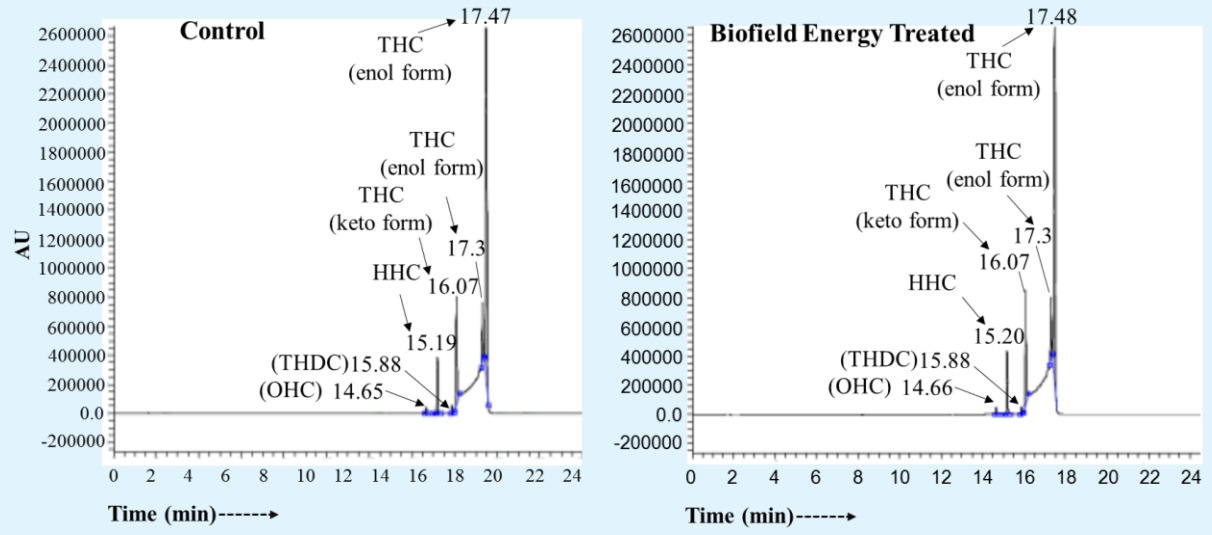

Figure 5: The LC chromatogram of the control and Biofield Energy Treated sample of THC.

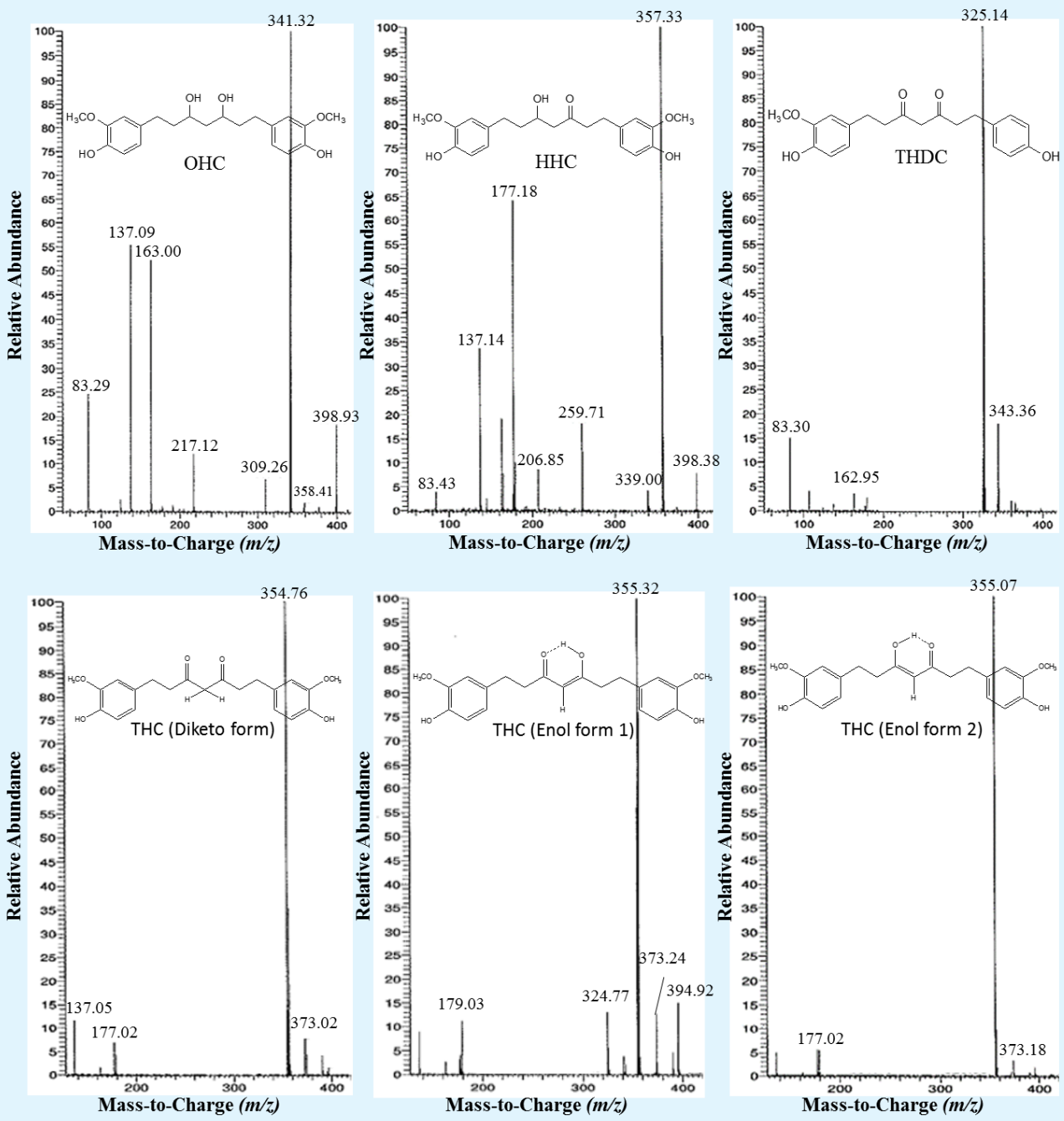

Figure 6: Mass spectra of the tetrahydrocurcumin (THC) and their proposed structures such as octahydrocurcumin (OHC), hexahydrocurcumin (HHC), tetrahydrodemethoxycurcumin (THDC), one diketo form of THC, and two enol forms of THC.

Peak	R_t (min)	m/z	Peak Area%		% Change*	Peak Intensity		% Change*
			Control	Biofield Treated		Control	Biofield Treated	
1	14.7	399	0.87	0.80	-8.05	219341	553367	152.29
2	15.2	398	8.46	8.40	-0.71	147388	690997	368.83
3	15.9	343	0.93	0.98	5.38	356587	335265	-5.98
4	16.1	373	17.28	17.56	1.62	1349539	1589661	17.79
5	17.3	373	7.90	7.26	-8.10	768568	1389643	80.81
6	17.5	373	64.30	64.74	0.68	976638	897169	-8.14

Table 2: The LC retention time (R_t), peak area% and mass peak intensity values for both the control and Biofield Energy Treated samples of THC *denotes the percentage change of the Biofield Energy Treated sample with respect to the control sample.

The existence of the three forms of THC (one diketo and two enol form) was also supported by the literature [8]. Literature demonstrated that the enol form of curcumin is the major form in solution [43]. Thus, THC (keto form) was proposed from the chromatographic peak at R_t of 16.1 minutes, which exhibited the mass of the molecular ion at *m/z* 373.02 $[M + H]^+$ (calculated for $C_{21}H_{25}O_6^+$, 373.16) in the control sample and at *m/z* 373.01 $[M + H]^+$ in the Biofield Energy Treated sample. The fragment ion peaks at *m/z* 354.76 and 355.07 (base peak) corresponded to the molecular formula $C_{21}H_{23}O_5^+$ (Figure 6) in control and Biofield Energy Treated samples, respectively supported the structure of THC. The chromatographic peak area% and the mass peak intensity of THC (keto form) were increased by 1.62% and 17.79%, respectively (Table 2). THC (enol form 1) was proposed from the chromatographic peak at R_t of 17.3 minutes, which exhibited the mass of the molecular ion at *m/z* 373.24 $[M + H]^+$ (calculated for $C_{21}H_{25}O_6^+$, 373.16) in the control sample and at *m/z* 373.04 $[M + H]^+$ in the Biofield Energy Treated sample. The fragment ion peaks at *m/z* 355.32 and 355.29 (base peak) corresponded to the molecular formula $C_{21}H_{23}O_5^+$ (Figure 6) in control and Biofield Energy Treated samples, respectively supported the structure of THC. The chromatographic peak area% of THC (enol form 2) was decreased by 8.10%, whereas the mass peak intensity was significantly increased by 80.81% (Table 2). Similarly, the THC (enol form 2) was proposed from the chromatographic peak at R_t of 17.3 minutes, which exhibited the mass of the molecular ion at *m/z* 373.18 $[M + H]^+$ (calculated for $C_{21}H_{25}O_6^+$, 373.16) in the control sample and at *m/z* 373.31 $[M + H]^+$ in the Biofield Energy Treated sample. The fragment ion peaks at *m/z* 355.07 and 354.92 (base peak) corresponded to the molecular formula $C_{21}H_{23}O_5^+$ (Figure 6) in control and Biofield Energy Treated samples, respectively supported the structure of THC. The chromatographic peak area% of THC (enol form 2) was increased by 0.68%, whereas the mass peak intensity was decreased by 8.14% (Table 2).

The liquid chromatograms revealed that the polarity of the Biofield Energy Treated sample did not change, but the peak area% and mass peak intensities were altered significantly compared with the control sample. The peak area is directly proportional to the relative concentration of the sample [44]. From the results, it can be assumed that the relative concentration of the Biofield Energy Treated THC was increased compared with the control sample (Table 2). The mass fragmentation pattern of both the control and Biofield Energy Treated samples showed a similar pattern. But, the mass peak intensity values (relative abundance) of the Biofield Energy Treated sample were significantly increased in most of the case compared with the control sample (Table 2). The altered relative abundance might affect the isotopic abundance ratio of Biofield Energy Treated THC. The relative abundances of an isotopic peak are the contributions of several different isotopes and its composition to the same peak [40]. The increased isotopic abundance ratio was supported by the GC-MS.

Nuclear Magnetic Resonance Spectroscopy (^1H & ^{13}C NMR)

The ^1H and ^{13}C NMR of the control and Biofield Energy Treated THC results are reports in Table 3. The characteristic proton signals for aromatic protons, $-CH_2$, $-OCH_3$ and -OH groups of THC in the ^1H NMR of spectra of both the control and Biofield Energy Treated samples were described (Table 3). Similarly, the characteristic carbon signals for –C=O, quaternary carbon (aromatic), -CH (aromatic), $-CH_2$, $-OCH_3$ groups of THC in the ^{13}C NMR of spectra of both the control and Biofield Energy Treated samples were described in Table 3. The results indicated that there was no such significant alternation in the

characteristic proton and carbon signals for THC in the ^{1}H and ^{13}C NMR spectrum of the Biofield Energy Treated sample as compared to the control sample.

Position	^{1}H NMR δ (ppm)		^{13}C NMR δ (ppm)	
	Untreated	Treated	Untreated	Treated
-OH (8,8')	8.67 (d, *J* = 8.8 Hz, 2H)	8.67 (d, *J* = 8.8 Hz, 2H)	--	--
-OCH_3 (9,9')	3.73 (s, 6H)	3.73 (s, 6H)	55.57	55.51
1	5.74 (1H, s)[a], 3.68 (2H, s)[b]	5.74 (1H, s)[a], 3.68 (2H, s)[b]	44.69, 44.77	44.71
2,2'	--	--	193.48, 204.78	193.39, 204.66
3,3'	2.74 (dd, *J* = 6.8, 14.4 Hz, 4H)	2.74 (dd, *J* = 6.4, 14.8 Hz, 4H)	30.52	30.46
4,4'	2.56 (t, *J* = 7.2, 8.4 Hz, 2H), 2.56 (t, 2H, dd, J = 15.6)[b]	2.56 (t, *J* = 7.2, 8 Hz, 2H)[a], 2.56 (t, 2H, dd, J = 15.2)[b]	28.45	28.39
5,5'	--	--	131.47, 131.69	131.36,131.59
6,6'	6.65 (dd, J = 3.2, 7.6 Hz, 2H)	6.65 (dd, J = 2.4, 8 Hz, 2H)	120.29, 120.35	120.21,120.27
7,7'	6.54-6.59 (m, 2H)	6.54-6.59 (m, 2H)	115.35	115.28
8,8'	--	--	147.46	144.60, 144.72
9,9'	--	--	144.64, 144.75	147.39
10,10'	6.76 (dd, *J* = 2, 13.6 Hz, 2H)	6.76 (dd, *J* = 1.6, 13.6 Hz, 2H)	112.47, 112.50	112.42, 112.46

Table 3: *NMR assignments of the control and Biofield Energy Treated Tetrahydrocurcumin.* s: singlet, d: doublet, dd: doublet of doublet, t: triplet, and m: multiplet, [a] enol form, [b]keto form.

Finally, GC-MS, LC-MS, and NMR study confirmed the structure of tetrahydrocurcuminoids (THC, OHC, HHC, and THDC), and the sample contains THC majorly. The GC-MS based isotopic abundance ratio of P_{M+1}/P_M ($^{2}H/^{1}H$ or $^{13}C/^{12}C$ or $^{17}O/^{16}O$) in the Biofield Energy Treated THC was increased compared to the control sample. According to modern physics, neutrinos change identities which are only possible if the neutrinos possess mass and have the ability to interchange their phase from one phase to another internally. Therefore, the neutrinos have the ability to interact with protons and neutrons in the nucleus, which indicated a close relation between neutrino and the isotope formation [36,45,46]. The Trivedi Effect® might alter the isotopic composition at the molecular level might be due to alteration in neutron to proton ratio in the nucleus. It is hypothesized that the changes in isotopic abundance could be due to changes in nuclei, possibly through the interference of neutrino particles *via* the Trivedi Effect®-Consciousness Energy Healing Treatment.

Conclusions

The experimental results revealed that the Trivedi Effect®-Consciousness Energy Healing Treatment showed a significant impact on the characteristic properties and isotopic abundance ratio of tetrahydrocurcumin. The spectroscopy study confirmed the structure of tetrahydrocurcuminoids (THC, octahydrocurcumin, hexahydrocurcumin, and tetrahydrodemethoxycurcumin) , and the sample majorly contains THC. The GC-MS and LC-MS of the control and Biofield Energy Treated samples revealed that the polarity of the Biofield Energy Treated sample was remained unaltered, but the chromatographic peak area% and mass peak intensities were notably altered compared to the control sample. The GC-MS spectra of the control and Biofield Energy Treated THC showed with the molecular ion at *m/z* 372.2 $(C_{21}H_{24}O_6)^+$ and the isotopic abundance ratio of P_{M+1}/P_M in the Biofield Energy Treated sample was increased by 2.12% compared with the control sample. Thus, the contributions of ^{13}C, ^{2}H, and ^{17}O from $(C_{21}H_{24}O_6)^+$ to *m/z* 373.2 in the Biofield Energy Treated sample were increased compared with the control sample. The LC-MS of both the sample exhibited three major peaks at R_t of 16.1, 17.3, and 17.48 minutes confirmed the presence of one diketo form and two enol form of THC, respectively. The peak area% of the Biofield Energy Treated THC at R_t of 16.1 and 17.5 minutes were increased by 1.62% and 0.68% respectively, whereas, at R_t of 17.30 minutes, it was decreased by 8.10% compared with the control sample. Similarly, the relative mass peak intensities of the Biofield Energy Treated THC at R_t of 16.1 and 17.3 minutes were significantly increased by 17.79% and 80.81% respectively, but at R_t of 17.5 minutes, it was decreased by 8.10% compared with the control sample. Thus, it can be assumed that the relative concentration of the Biofield Energy Treated THC was altered compared

with the control sample. Therefore, the Trivedi Effect®-Consciousness Energy Healing Treated THC with improved isotopic abundance ratio and relative concentration might have altered the solubility, bioavailability, and thermal stability compared to the untreated THC. The Biofield Energy Treated THC would be very useful to design better nutraceutical and pharmaceutical formulations which might offer better therapeutic response against various inflammatory diseases, dementia, arthritis, cancer, diabetes, nephrotoxicity, hepatotoxicity, ageing process, psoriasis, scleroderma, atherosclerotic lesions treatment, tumors of skin, colon, pancreas, and breast.

Acknowledgements

The authors are grateful to GVK Biosciences Pvt. Ltd., Trivedi Science, Trivedi Global, Inc., Trivedi Testimonials, and Trivedi Master Wellness for their assistance and support during this work.

References

1. GM Holder, JL Plummer, AJ Ryan (1978) Metabolism and excretion of curcumin (1,7-bis-(4-hydroxy-3-methoxyphenyl)-1,6-heptadiene-3,5-dione) in the rat. Xenobiotica 8(12): 761-768.

2. Aggarwal BB, Deb L, Prasad S (2014) Curcumin differs from tetrahydrocurcumin for molecular targets, signaling pathways and cellular responses. Molecules 20(1): 185-205.

3. Lai CS, Wu JC, Yu SF, Badmaev V, Nagabhushanam K, et al. (2011) Tetrahydrocurcumin is more effective than curcumin in preventing azoxymethane-induced colon carcinogenesis. Mol Nutr Food Res 55(12): 1819-1828.

4. Yoysungnoen P, Wirachwong P, Changtam C, Suksamrarn A, Patumraj S (2008) Anti-cancer and anti-angiogenic effects of curcumin and tetrahydrocurcumin on implanted hepatocellular carcinoma in nude mice. World J Gastroenterol 14(13): 2003-2009.

5. Park S, Lee LR, Seo JH, Kang S (2016) Curcumin and tetrahydrocurcumin both prevent osteoarthritis symptoms and decrease the expressions of pro-inflammatory cytokines in estrogen-deficient rats. Genes Nutr 11: 2.

6. Naito M, Wu X, Normura H, Kodama M, Kato Y, et al. (2002) The protective effect of tetrahydrocurcumin on oxidative stress in cholesterol-fed rabbits. J Atheroscler Thromb 9(5): 243-250.

7. Wu JC, Tsai ML, Lai CS, Wang YJ, Ho CT, et al. (2014) Chemopreventative effects of tetrahydrocurcumin on human diseases. Food Funct 5(1): 12-27.

8. Girija CR, Begum NS, Syed AA, Thiruvenkatam V (2004) Hydro-gen-bonding and C-H...[π] interactions in 1,7-bis(4-hydroxy-3-methoxy-phenyl)-heptane-3,5-dione (tetra-hydro-curcumin). Acta Crystallographica Section C: Crystal Structure Communications 60(pt8): o611-o613.

9. Setthacheewakul S, Kedjinda W, Maneenuan D, Wiwattanapatapee R (2011) Controlled release of oral tetrahydrocurcumin from a novel self-emulsifying floating drug delivery system (SEFDDS). AAPS PharmSciTech 12(1): 152–164.

10. Neyrinck AM, Alligier M, Memvanga PB, Nevraumont E, Larondelle Y, et al. (2013) *Curcuma longa* extract associated with white pepper lessens high fat diet-induced inflammation in subcutaneous adipose tissue. PLoS One 8(11): e81252.

11. Trivedi MK, Tallapragada RM, Branton A, Trivedi D, Nayak G, et al. (2015) Potential impact of biofield treatment on atomic and physical characteristics of magnesium. Vitam Miner 3: 129.

12. Trivedi MK, Tallapragada RM, Branton A, Trivedi D, Nayak G, et al. (2015) Physicochemical characterization of biofield energy treated calcium carbonate powder. American Journal of Health Research 3(6): 368-375.

13. Rubik B (2002) The biofield hypothesis: Its biophysical basis and role in medicine. J Altern Complement Med 8(6): 703-717.

14. Nemeth L (2008) Energy and biofield therapies in practice. Beginnings 28(3): 4-5.

15. Rivera-Ruiz M, Cajavilca C, Varon J (2008) Einthoven's string galvanometer: The first electrocardiograph. Tex Heart Inst J 35(2): 174-178.

16. Koithan M (2009) Introducing complementary and alternative therapies. J Nurse Pract 5(1): 18-20.

17. Trivedi MK, Branton A, Trivedi D, Nayak G, Mondal SC, et al. (2015) Morphological characterization, quality,

yield and DNA fingerprinting of biofield energy treated alphonso mango (*Mangifera indica* L.). Journal of Food and Nutrition Sciences 3(6): 245-250.

18. Trivedi MK, Branton A, Trivedi D, Nayak G, Mondal SC, et al. (2015) Evaluation of plant growth, yield and yield attributes of biofield energy treated mustard (*Brassica juncea*) and chick pea (*Cicer arietinum*) seeds. Agriculture, Forestry and Fisheries 4(6): 291-295.

19. Trivedi MK, Branton A, Trivedi D, Nayak G, Mondal SC, et al. (2015) Evaluation of plant growth regulator, immunity and DNA fingerprinting of biofield energy treated mustard seeds (*Brassica juncea*). Agriculture, Forestry and Fisheries 4(6): 269-274.

20. Trivedi MK, Patil S, Shettigar H, Mondal SC, Jana S (2015) *In vitro* evaluation of biofield treatment on *Enterobacter cloacae*: Impact on antimicrobial susceptibility and biotype. J Bacteriol Parasitol 6(5): 241.

21. Trivedi MK, Patil S, Shettigar H, Mondal SC, Jana S (2015) Evaluation of biofield modality on viral load of Hepatitis B and C Viruses. J Antivir Antiretrovir 7(3): 083-088.

22. Trivedi MK, Patil S, Shettigar H, Mondal SC, Jana S (2015) An impact of biofield treatment: Antimycobacterial susceptibility potential using BACTEC 460/MGIT-TB System. Mycobact Dis 5(4): 189.

23. Trivedi MK, Branton A, Trivedi D, Nayak G, Mondal SC, et al. (2015) Antimicrobial sensitivity, biochemical characteristics and biotyping of *Staphylococcus saprophyticus*: An impact of biofield energy treatment. J Women's Health Care 4(6): 271.

24. Trivedi MK, Branton A, Trivedi D, Nayak G, Mondal SC, et al. (2015) Evaluation of antibiogram, genotype and phylogenetic analysis of biofield treated *Nocardia otitidis*. Biol Syst Open Access 4(2): 143.

25. Trivedi MK, Branton A, Trivedi D, Nayak G, Charan S, et al. (2015) Phenotyping and 16S rDNA analysis after biofield treatment on *Citrobacter braakii*: A urinary pathogen. J Clin Med Genom 3: 129.

26. Trivedi MK, Patil S, Shettigar H, Mondal SC, Jana S (2015) The potential impact of biofield treatment on human brain tumor cells: A time-lapse video microscopy. J Integr Oncol 4(3): 141.

27. Trivedi MK, Patil S, Shettigar H, Gangwar M, Jana S (2015) *In vitro* evaluation of biofield treatment on cancer biomarkers involved in endometrial and prostate cancer cell lines. J Cancer Sci Ther 7: 253-257.

28. Trivedi MK, Nayak G, Patil S, Tallapragada RM, Latiyal O, et al. (2015) Impact of biofield treatment on atomic and structural characteristics of barium titanate powder. Ind Eng Manage 4: 166.

29. Trivedi MK, Patil S, Nayak G, Jana S, Latiyal O (2015) Influence of biofield treatment on physical, structural and spectral properties of boron nitride. J Material Sci Eng 4: 181.

30. Trivedi MK, Nayak G, Patil S, Tallapragada RM, Latiyal O, et al. (2015) Characterization of physical and structural properties of brass powder after biofield treatment. J Powder Metall Min 4: 134.

31. Trivedi MK, Branton A, Trivedi D, Nayak G, Nykvist CD, et al. (2017) Evaluation of the Trivedi Effect®-Energy of Consciousness Energy Healing Treatment on the physical, spectral, and thermal properties of zinc chloride. American Journal of Life Sciences. 5(1): 11-20.

32. Trivedi MK, Branton A, Trivedi D, Nayak G, Lee AC, et al. (2017) investigation of physicochemical, spectral, and thermal properties of sodium selenate treated with the Energy of Consciousness (the Trivedi Effect®). American Journal of Life Sciences 5(1): 27-37.

33. Trivedi MK, Branton A, Trivedi D, Nayak G, Wellborn BD, et al. (2017) Characterization of physicochemical, thermal, structural, and behavioral properties of magnesium gluconate after treatment with the Energy of Consciousness. International Journal of Pharmacy and Chemistry 3(1): 1-12.

34. Trivedi MK, Branton A, Trivedi D, Nayak G, Panda P, et al. (2016) Isotopic abundance ratio analysis of 1,2,3-trimethoxybenzene (TMB) after biofield energy treatment (the Trivedi Effect®) using gas chromatography-mass spectrometry. American Journal of Applied Chemistry 4(4): 132-140.

35. Trivedi MK, Branton A, Trivedi D, Nayak G, Sethi KK, et al. (2016) Gas chromatography-mass spectrometry based isotopic abundance ratio analysis of biofield energy treated methyl-2-napthylether (Nerolin). American Journal of Physical Chemistry 5(4): 80-86.

36. Trivedi MK, Mohan TRR (2016) Biofield energy signals, energy transmission and neutrinos. American Journal of Modern Physics 5(6): 172-176.

37. Schellekens RC, Stellaard F, Woerdenbag HJ, Frijlink HW, Kosterink JG (2011) Applications of stable isotopes in clinical pharmacology. Br J Clin Pharmacol 72(6): 879-897.

38. Weisel CP, Park S, Pyo H, Mohan K, Witz G (2003) Use of stable isotopically labeled benzene to evaluate environmental exposures. J Expo Anal Environ Epidemiol 13(5): 393-402.

39. Rosman KJR, Taylor PDP (1998) Isotopic compositions of the elements 1997 (Technical Report). Pure Appl Chem 70(1): 217-235.

40. Smith RM (2004) Understanding Mass Spectra: A Basic Approach, 2nd (Edn.), John Wiley & Sons.

41. Jürgen H (2004) Gross Mass Spectrometry: A Textbook (2nd Edn) Springer: Berlin.

42. Trivedi MK, Branton A, Trivedi D, Nayak G, Sethi KK, et al. (2016) Evaluation of isotopic abundance ratio in biofield energy treated nitrophenol derivatives using gas chromatography-mass spectrometry. American Journal of Chemical Engineering 4(3): 68-77.

43. Kawano SI, Inohana Y, Hashi Y, Lin JM (2013) Analysis of keto-enol tautomers of curcumin by liquid chromatography/mass spectrometry. Chin Chem Lett 24(8): 685–687.

44. Andrew Berry, Theory-of-HPLC-Quantitative-and-Qualitative-HPLC.

45. www.nobelprize.org/nobel_prizes/physics/laureates /2015/advanced-physicsprize2015. pdf.

46. Balantekin AB (2013) Neutrinos and rare isotopes. Journal of Physics: Conference Series 445: 012022.